Magnetic Susceptibility as a Proxy for Investigating Microbial Mediated Iron Reduction

Farag M. Mewafy[1,2], Estella A. Atekwana[1*], D. Dale Werkema Jr.[3], Lee D. Slater [4]

Dimitrios Ntarlagiannis[4], André Revil[5,6], Magnus Skold[5], Geoffrey N. Delin[7]

1. *Oklahoma State University, Stillwater, OK 74078*
2. *Geology Department, Faculty of Science, Assiut University, Assiut,71515, Egypt*
3. *U.S. Environmental Protection Agency, Las Vegas, NV 89119*
4. *Department of Earth & Environmental Sciences, Rutgers-Newark, NJ 07102*
5. *Department of Geophysics, Colorado School of Mines, Golden, CO 80401*
6. *ISTerre, CNRS, UMR 5559, Université de Savoie, Le Bourget du Lac, France*
7. *U.S. Geological Survey, Denver Federal Center, MS406; Denver, CO 80225.*

Corresponding author: Tel.: +1 405 744 6358; Fax: +1 405 744 7841

Email address: estella.atekwana@okstate.edu

Abstract. We investigated magnetic susceptibility (MS) variations in hydrocarbon contaminated sediments. Our objective was to determine if MS can be used as an intrinsic bioremediation indicator due to the activity of iron-reducing bacteria. A contaminated and an uncontaminated core were retrieved from a site contaminated with crude oil near Bemidji, MN and subsampled for MS measurements. The contaminated core revealed enriched MS zones within the hydrocarbon smear zone, which is related to iron-reduction coupled to oxidation of hydrocarbon compounds and the vadose zone, which is coincident with a zone of methane depletion suggesting aerobic or anaerobic oxidation of methane is coupled to iron-reduction. The latter has significant implications for methane cycling. We conclude that MS can serve as a proxy for intrinsic bioremediation by iron-reducing bacteria and for the application of geophysics to iron cycling studies.

INDEX TERMS: 0925 Magnetic and electrical methods, 0416 Biogeophysics, 0463 Microbe/mineral interactions, 0418 Bioremediation.

1.0 Introduction

The Deepwater Horizon spill in the Gulf of Mexico is a reminder of the environmental threat of hydrocarbon contamination and the need for technological advancements for detecting,

monitoring, and remediating hydrocarbon contamination. Due to the relationship between magnetic minerals and redox reactions associated with hydrocarbon seeps, magnetic susceptibility (MS) has been used as a possible tool for oil exploration [e.g., *Saunders et al.*, 1999]. In surficial sediments, MS traditionally is used for climate studies [e.g., *Kukla et al.*, 1988], mapping heavy metal soil contamination [e.g., *Hanesch and Scholger*, 2002], and identifying sediment sources and transport trends [*Ellwood et al.*, 2006]. MS has recently emerged as a tool for investigating iron cycling mediated by microbial activity [e.g., *Porsch et al.*, 2010;*Rijal et al.*, 2010].

This work investigates MS variations in a hydrocarbon contaminated aquifer where methanogenesis and iron-reduction are the main terminal electron acceptor processes [*Baedecker et al.,* 1993]. Our objective was to determine if MS could be an indicator of the presence of intrinsic hydrocarbon bioremediation by iron-reducing bacteria. Our results suggest enhancements in MS are due to the precipitation of magnetite coupled to iron-reduction as related to; (1) anaerobic oxidation of hydrocarbon compounds within the smear zone and (2) aerobic or anaerobic oxidation of methane within the vadose zone, which provides additional field evidence linking anaerobic oxidation of methane to iron-reduction and suggests significant implications for methane cycling in terrestrial environments.

1.1 Site History

The National Crude Oil Spill Fate and Natural Attenuation Research Site at Bemidji, MN (Figure 1), is a field laboratory for investigating biogeophysical signatures associated with the intrinsic bioremediation of a crude oil spill. In August 1979, a high pressure crude oil pipeline ruptured, releasing 1,700,000 L of crude oil. Oil pooled in low-lying areas (~2000 m^2) over a total area of 6,500 m^2 to the southwest of the pipeline forming the south and north contaminated

plumes. The study site consists of ~ 20 m-thickness of moderately calcareous silty sand and outwash glacial deposits overlying clayey till of unknown thickness [*Bennett et al.*, 1993]. The north plume has been the focus of intensive geochemical [e.g., *Cozzarelli et al.*, 2010 and references therein] and microbiological studies [e.g., *Bekins et al.*, 2001].

The uncontaminated groundwater is aerobic with dissolved oxygen concentrations between 8 and 9 mg/L, dissolved organic carbon of 2.8 mg/L as C, and low levels of nitrate at 44.8 μg/L as N_2, and sulfate at 2.9 mg/L [*Bennett et al.*, 1993]. Geochemical changes in the subsurface plume have been previously described by *Baedecker et al.* [1993] and *Cozzarelli et al.* [2010]. The aquifer is divided in the vicinity of the oil body into anoxic, transition, and background zones. In the anoxic portion, hydrocarbons are oxidized predominantly by iron reduction [*Lovley et al.*, 1989] and methanogenesis [*e.g., Baedecker et al., 1993*]. *Bekins et al.* [2001] show two zones of methanogenic activity with CH_4 concentrations greater than 15 mg/L. The vadose zone vapor plume near the oil body has low O_2 concentrations (< 2%) and high levels of CO_2 (>10%) and CH_4 (>15%). Four physiologic microbial populations within the anaerobic portion of the contaminated aquifer suggest the progression from iron-reduction to methanogensis [*Bekins et al.* 2001].

2.0 Materials and Methods

2.1 Retrieval of Cores

Two ~5-cm diameter cores were retrieved from contaminated (C1010) and uncontaminated (C1006) locations (Figure 1). In the uncontaminated location two segments of core were collected, representing the vadose and saturated zones. The cores were collected by advancing a core barrel with a polycarbonate liner ahead of a hollow-stem auger. The cores within the smear zone or below the water table were collected with a freezing drive shoe [*Murphy and Herkelrath*,

77 1996], preserved in coolers unexposed to the atmosphere, and expeditiously shipped to the
78 laboratory at Oklahoma State University.

79 **2.2 MS Measurements and Iron Analysis**

80 Sub-samples of ~10 grams were taken at 5 to 15 cm intervals along the cores. Sub-samples
81 were oven dried at 50°C for 24 hours then analyzed for MS using a Bartington MS2 magnetic
82 susceptibility meter (1.2566 x 10-11 m3/kg sensitivity). Then the same samples were used to
83 quantify iron content. The mass of magnetic particles retained by a bar magnet was measured
84 and the percentage of the iron-rich material per sample was determined.

85 **2.3 Gas data**

86 Vapor wells, 534 (contaminated) and 310 (uncontaminated) (Fig 1) consisted of permanently
87 installed vapor probes generally spaced at 50- to 100-cm depth intervals in the unsaturated zone,
88 from 1 m below land surface to 1 m above the water table. Each probe was constructed of 0.16-
89 to 0.64-cm outside diameter stainless steel tubing with 5 to 10-cm long screens at the bottom.
90 The probes were installed in 10-cm-diameter augered holes, which were backfilled with native
91 sand, and included a bentonite seal between each screened interval. The gas samples were
92 obtained in gas-tight glass syringes using a peristaltic pump and analyzed on-site using a SRI®
93 8610C Gas Chromatograph (GC). The GC was configured using a 1.0-mL fixed-loop injection
94 and an internal air compressor. Fixed gas (Ar, O_2, CO_2, and CH_4) analyses were determined with
95 a thermal conductivity detector (TCD) and a SRI® CTR-1 double-packed column.
96 Concentrations of gases were quantified in weight percent using gas standards containing
97 mixtures of Ar, O_2, CO_2, and CH_4.

98 **3.0 Results**

99 **3.1 Magnetic Susceptibility**

The contaminated core shows two zones of higher MS (Figure 2a) versus the uncontaminated core (Figure 3a). The first zone is located from ~423 m elevation at the base of the free hydrocarbon to 426 m at the top of the groundwater table (GWT) where the MS values range from 75 to 299 $x10^{-8}$ m^3kg^{-1} reaching a maximum at 423.5 m(Figure 2c). The second zone is between 428-429 m where the MS values range between 88 to $218x10^{-8}$ m^3kg^{-1} to a maximum at ~429 m (Figure 2a). Another zone of high MS is observed at 427.2 m. These high MS zones occur within the vadose zone with no corresponding free or residual hydrocarbon contamination (Figure 2c). The MS of the uncontaminated cores show relatively small variations with no anomalous zones and values ranging from 40 to $145x10^{-8}$ $m^3.kg^{-1}$ (Figure 3a).

3.2 Magnetic minerals analysis

The magnetic mineral concentration data in the uncontaminated core show no anomalous concentrations with values ranging from $0.76x10^{-3}$ ppm to $2.2x10^{-3}$ ppm and an average value of $1.48x10^{-3}$ ppm. In contrast, the contaminated core shows elevated concentrations between $1.9x10^{-3}$ ppm to $4.4x10^{-3}$ ppm, reaching a maximum at 423.5 m at depths coincident with higher MS (Figure 2b). In the 428-430 m elevation interval, the concentration of magnetic minerals ranges between $1.9x10^{-3}$ ppm to $4.2x10^{-3}$ ppm with a maximum at 429 m. The correlation between MS and magnetite suggest that magnetite is responsible for the MS variations with an R^2 of 0.817 and 0.967 for the contaminated and uncontaminated cores, respectively. An XRD profile (data not shown) suggested that magnetite was the dominant phase.

3.3 Distribution of Ar + O_2, CH_4 and CO_2

The 2005 CO_2 gas data increases downward from nearly 0.7% at ground surface to 6.5% at 430 m and 12.2% at 429 m. Ar and O_2 decrease downward to less than 11.9% at 430 m to 2.9% at 429 m and are depleted at 428 m. CH_4 shows depletion upwards from about 4% at 427m to 0%

123 at 429 m(Figure 2d). These data define a transition zone from ~427 m to 430 m where O_2 and
124 CH_4 are depleted and CO_2 is enriched. The same trends occur in the 2010 data; however, the
125 transition zone has shifted to a lower elevation (Figure 2e). The uncontaminated gas
126 concentration profile shows no variability and gas concentrations are equal to atmospheric
127 values.

128 **4.0 Discussion and Conclusions**

129 The MS and magnetic mineral concentration differed between the contaminated and
130 uncontaminated cores. An upper zone, between 428- 430 m, and a lower zone, between 423-426
131 m of enhanced magnetite formation were observed.

132 **4.1 Mechanisms for Magnetite Formation**

133 Geochemical and microbial studies suggest iron reduction is an important terminal electron
134 acceptor process occurring within the anaerobic plume [e.g. *Baedecker et al.*, 1993]. In addition,
135 iron-reducing bacteria such as *Geobacter bemidjiensis sp. and Geobacter psychrophilus sp* occur
136 in the contaminated aquifer [*Nevin et al.*, 2005]. During iron reduction, Fe(III) is converted to
137 Fe(II):

138 $Fe_2O_3 + 3H_2 \rightarrow 2Fe(OH)_2 + H_2O$ ……..……(1).

139 The ferrous hydroxide ($Fe(OH)_2$) can be oxidized by the protons of water to form magnetite and
140 molecular hydrogen:

141 $3\ Fe(OH)_2 \rightarrow Fe_3O_4\downarrow + H_2 + 2\ H_2O$……..……(2).

142 **4.2 Smear Zone**

143 The contaminated core smear zone above the GWT (423.5-425 m) shows the highest MS
144 values and concentration of magnetite recorded (Figure 2a-c). Biogeophysical investigations at
145 other hydrocarbon contaminated sites have documented the highest value of bulk electrical

146 conductivity within this smear zone and suggested it to be most biologically active [*Werkema et*
147 *al.*, 2003]. Additionally, MS studies by *Rijal et al.* [2010] show concentrations of magnetic
148 parameters increasing towards the top of the GWT. Thus, we infer this enriched zone of
149 magnetite is due to the anaerobic oxidation of hydrocarbons by iron-reducing bacteria [*Lovley et*
150 *al.*, 1989]. Microbial data showed culturable iron reducers were present in the oil layer in 1997
151 [*Bekins et al.*, 1999].

152 **4.3 Unsaturated zone**

153 The zone of enriched magnetite occurring in the vadose zone (428-430 m) (Figure 2a) can be
154 explained by: (1) naturally occurring higher concentration of magnetite within the sediments in
155 this zone, (2) precipitation of magnetite (eq. 2 and 3) related to past hydrocarbon vapors in the
156 vadose zone, (3) precipitation of magnetite (eq. 2), related to aerobic oxidation of methane (eq.
157 3) which releases water protons that can oxidize Fe $(OH)_2$ to magnetite,

158 $CH_4 + 2O_2 \rightarrow CO_2 + 2H_2O$…….....…….……(3).

159 or (4) the precipitation of magnetite resulting from anaerobic oxidation of methane (AOM)
160 coupled to iron reduction.

161 Although there are presently no hydrocarbon vapors present in the vadose zone, vapors were
162 present in the past [*Chaplin et al*. 2002]. Hence, the zone of enriched magnetite occurring in the
163 vadose zone at the 428-430 m elevation (Figure 2a) could represent a relict process of bacterial
164 oxidation of the hydrocarbon vapors coupled to iron reduction. Nevertheless, we favor
165 hypotheses 3 and 4 for the following reason. The gas data (Figures 2d-e) suggest a transition in
166 the methane and oxygen plots crossing at 428.3 m (2005) and 427.2 m (2010), where the total
167 depletion of methane occurs. Also, culturable methanotroph microbial population numbers peak
168 within this zone [*Molins et al.,* 2010; data not shown]. This has led some to suggest the aerobic

169 oxidation of methane within this zone [*Amos et al.,* 2005]. It is possible that the precipitation of
170 magnetite in this zone could be linked to the aerobic oxidation of methane (eq. 2 and 3).

171 The precipitation of magnetite resulting from the anaerobic oxidation of methane (AOM)
172 coupled to iron reduction is also possible. Whereas AOM coupled to sulfate reduction is
173 documented in marine environments [e.g., *Hoehler et al.*, 1994], AOM coupled to metal
174 reduction is not common and has yet to be definitively demonstrated. There are also no known
175 microorganisms capable of this process [*Beal et al.,* 2009]. Nonetheless, recent studies postulate
176 that AOM coupled to metal reduction is likely to occur [e.g., *Beal et al.,* 2009; *Crowe et al.,*
177 2011]. *Beal et al.* [2009] show AOM in the absence of sulfate if birnessite or ferrihydrite is
178 present. *Crowe et al.*, [2011] document that, despite high abundances of Fe (hydr)oxides in lake
179 sediments, more than 50% of antigenic organic matter was degraded through methanogenesis,
180 suggesting methane oxidation and Fe(III) reduction coupling. This mechanism is as follows:
181 (1) AOM coupled with ferrihydrite (simplified as $Fe(OH)_3$) reduction [*Beal et al.*, 2009].
182 $CH_4+8Fe(OH)_3+ 15H^+ \rightarrow HCO_3^- +8Fe^{2+}+ 21H_2O$ ……..(4).
183 Part of the Fe^{2+} reacts with the small amounts of O_2 present, thereby precipitating magnetite:
184 $3\ Fe(OH)_2 + ½\ O_2 \rightarrow Fe(OH)_2.2\ FeOOH + H_2O$ ……..……(5).
185 $Fe(OH)_2.2\ FeOOH \rightarrow Fe_3O_4\downarrow + 2H_2O$ …..……..…….(6).
186 The remaining ferrous hydroxide $Fe(OH)_2$ can be oxidized by water protons to form magnetite
187 and molecular hydrogen (eq. 2).

188 Geochemical studies at this site show low levels of nitrate (44.8 µg/L as N_2) and sulfate (2.9
189 mg/L) [*Bennett et al.*, 1993], which, in addition to elevated precipitation of magnetite, supports
190 our argument that this is a zone of methane oxidation coupled with iron reduction. Our study
191 suggests that MS measurements may aid in field investigations of this process. AOM coupled to

192 iron reduction has significant implications for methane cycling in terrestrial environments.
193 Biogeophysical studies can help guide microbial sampling thereby advancing microbial ecology
194 studies of new microbial species associated with bioremediation.

195 **Acknowledgements**

196 This material is partially based on work supported by Enbridge Energy (Ltd.), the Minnesota
197 Pollution Control Agency, and the U.S.G.S. Toxic Waste Substances Program. We thank W.
198 Herkalrath, F. Day-Lewis, J. Lane, M. Erickson, and J. Trost (U.S.G.S.), J. Heenan and C. Zhang
199 (Rutgers-Newark) for valuable field support. B. Bekins and I. Cozzarelli (U.S.G.S) reviewed an
200 earlier version of the manuscript. The U.S. EPA Office of Research and Development funded
201 and collaborated in the research described here under EP-10-D-000488. It has been subjected to
202 Agency review and approved for publication.

203 **References**

204 Amos, R.T., Mayer, K.U., Bekins, B.A., Delin, G.N., Williams, R.L. (2005), Use of dissolved
205 and vapor-phase gases to investigate methanogenic degradation of petroleum hydrocarbon
206 contamination in the subsurface, *Water Resources Research*, 41(2), W02001

207 Baedecker, M. J., I. M. Cozzarelli, R. P. Eganhouse, D. I. Siegel, and P. C. Bennett (1993),
208 Crude-oil in a shallow sand gravel aquifer 3. Biogeochemical reactions and mass-balance
209 modelling in anoxic groundwater, *Applied Geochemistry*, *8*(6), 569-586.

210 Beal, E. J., C. H. House, and V. J. Orphan (2009), Manganese- and Iron-Dependent Marine
211 Methane Oxidation, *Science*, *325*(5937), 184-187.

212 Bekins, B.A., Godsy, E.M., Warren, E., (1999). Distribution of microbial physiologic types in an
213 aquifer contaminated by crude oil, *Microbial Ecology* 37, 263–275.

214 Bekins, B. A., I. M. Cozzarelli, E. M. Godsy, E. Warren, H. I. Essaid, and M. E. Tuccillo (2001),
215 Progression of natural attenuation processes at a crude oil spill site: II. Controls on spatial
216 distribution of microbial populations, *Journal of Contaminant Hydrology*, *53*(3-4), 387-406.
217 Bennett, P. C., D. E. Siegel, M. J. Baedecker, and M. F. Hult (1993), Crude oil in a shallow sand
218 and gravel aquifer—I. Hydrogeology and inorganic geochemistry, *Applied Geochemistry*,
219 *8*(6), 529-549.
220 Chaplin, B. P., G. N. Delin, R. J. Baker, and M. A. Lahvis (2002), Long-term evolution of
221 biodegradation and volatilization rates in a crude oil-contaminated aquifer, *Bioremediation*
222 *Journal*, *6*, 237-255.
223 Cozzarelli, I. M., B. A. Bekins, R. P. Eganhouse, E. Warren, and H. I. Essaid (2010), In situ
224 measurements of volatile aromatic hydrocarbon biodegradation rates in groundwater, *Journal*
225 *of Contaminant Hydrology*, *111*(1-4), 48-64.
226 Crowe, S. A., et al. (2011), The methane cycle in ferruginous Lake Matano, *Geobiology*, 9(1),
227 61-78.
228 Ellwood, B. B., W. L. Balsam, and H. H. Roberts (2006), Gulf of Mexico sediment sources and
229 sediment transport trends from magnetic susceptibility measurements of surface samples,
230 *Marine Geology*, *230*(3-4), 237-248.
231 Hanesch, and Scholger (2002), Mapping of heavy metal loadings in soils by means of magnetic
232 susceptibility measurements, *Environmental Geology*, *42*(8), 857-870.
233 Hoehler, T. M., M. J. Alperin, D. B. Albert, and C. S. Martens (1994), Field and laboratory
234 studies of methane oxidation in an anoxic marine sediment: Evidence for a methanogen-
235 sulfate reducer consortium, *Global Biogeochemical Cycles*, 8(4), 451-463.

236 Kukla, G., F. Heller, L. X. Ming, X. T. Chun, L. T. Sheng, and A. Z. Sheng (1988), Pleistocene
237 climates in China dated by magnetic susceptibility, *Geology*, *16*(9), 811-814.
238 Lovley, D. R., M. J. Baedecker, D. J. Lonergan, I. M. Cozzarelli, E. J. P. Phillips, and D. I.
239 Siegel (1989), Oxidation of aromatic contaminants coupled to microbial iron reduction,
240 *Nature*, *339*(6222), 297-300.
241 Molins, S., K.U. Mayer, R.T. Amos, and B.A. Bekins (2010), Vadose zone attenuation of
242 volatile organic compounds at a crude oil spill site – Interactions between multicomponent
243 gas transport and biogeochemical reactions, *Journal of Contaminant Hydrology*, 112, 15-29.
244 Murphy, F., Herkelrath, W.N., (1996), A sample-freezing drive shoe for a wire line piston core
245 sampler, *Ground Water Monitoring and Remediation* 16, 86-90.
246 Nevin, K. P., D. E. Holmes, T. L. Woodard, E. S. Hinlein, D. W. Ostendorf, and D. R. Lovley
247 (2005), Geobacter bemidjiensis sp. nov. and Geobacter psychrophilus sp. nov., two novel
248 Fe(III)-reducing subsurface isolates, *International Journal of Systematic and Evolutionary*
249 *Microbiology*, *55*(4), 1667-1674.
250 Porsch, K., U. Dippon, M. L. Rijal, E. Appel, and A. Kappler (2010), In-situ magnetic
251 susceptibility measurements as a tool to follow geomicrobiological transformation of Fe
252 minerals, *Environmental Science & Technology*, *44*(10), 3846-3852.
253 Rijal, M. L., E. Appel, E. Petrovský, and U. Blaha (2010), Change of magnetic properties due to
254 fluctuations of hydrocarbon contaminated groundwater in unconsolidated sediments,
255 *Environmental Pollution*, *158*(5), 1756-1762.
256 Saunders, D. F., K. R. Burson, and C. K. Thompson (1999), Model for hydrocarbon
257 microseepage and related near-surface alterations, *American Association of Petroleum*
258 *Geologists Bulletin*, *83*(1), 170-185.

259 Werkema, D. D., Jr., E. A. Atekwana, A. L. Endres, W. A. Sauck, and D. P. Cassidy (2003),
260 Investigating the geoelectrical response of hydrocarbon contamination undergoing
261 biodegradation, *Geophys. Res. Lett.*, *30*(12), 1647.

262 **Figure Captions**

263 Figure 1. Study area showing the location of core samples (circles) and gas data (triangles) at
264 contaminated (closed symbols) and uncontaminated (opened symbols) boreholes. 310 and
265 534 are vadose zone gas sampling boreholes.

266 Figure 2. (a) Magnetic susceptibility, (b) concentration of magnetic minerals, (c) hydrocarbon
267 distribution within core, gas concentrations in (d) 2005, and (e) 2010 along the
268 contaminated core (C 1010). HWT: Highest water level, LWT: Lowest water level and
269 WT: Water Table during the time of measurements. Elevation above mean sea level (amsl).
270 The gas data are from location 534 located 10 m from C1010.

271 Figure 3. (a) Magnetic susceptibility, (b) concentration of magnetic minerals, and (c)
272 hydrocarbon distribution in two 2-m zones along the uncontaminated borehole (C 1006).
273 WT: Water Table during the time of measurements. Elevation above mean sea level (amsl).

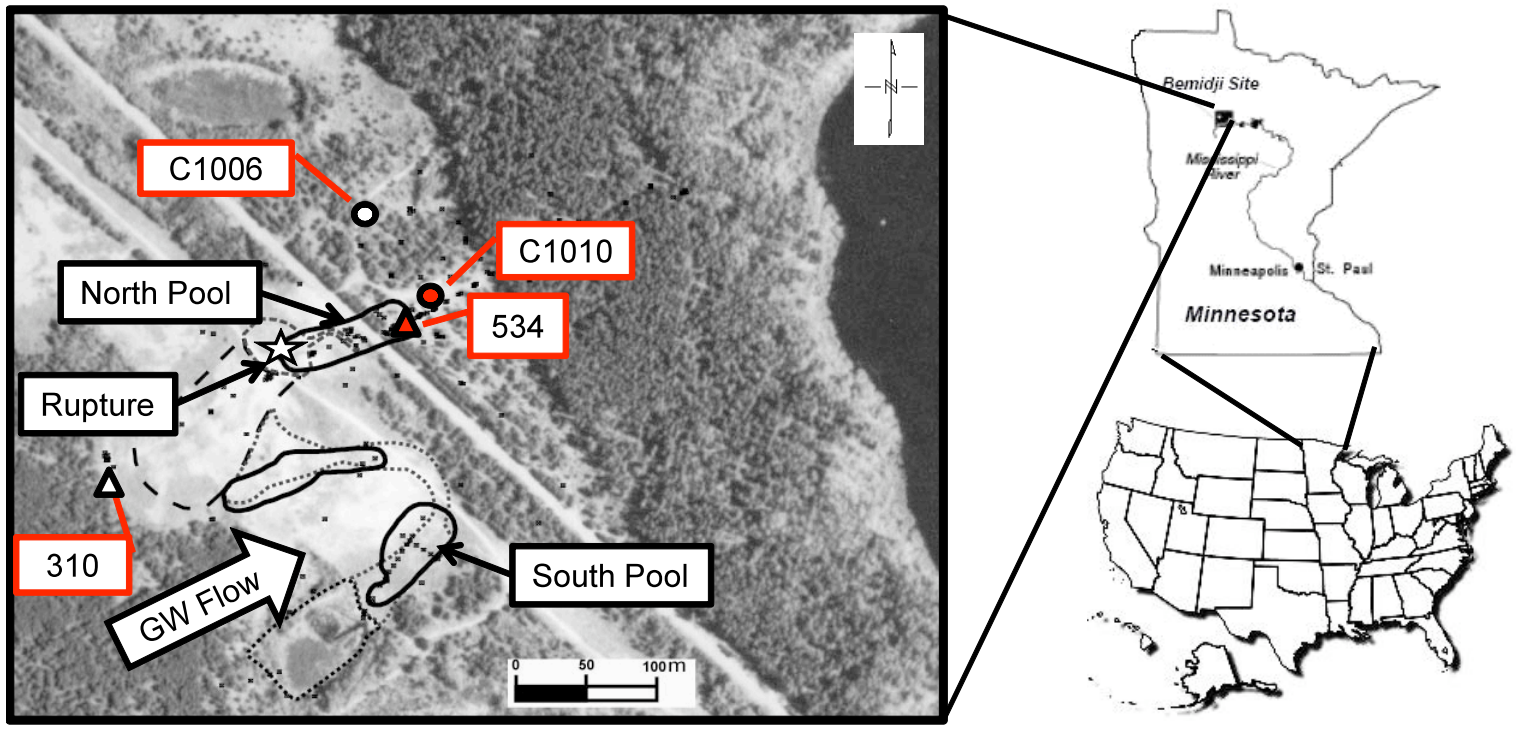
C1006
C1010
North Pool
534
Rupture
310
GW Flow
South Pool
0
50
100m
Bemidji Site
Minneapolis
St. Paul
Minnesota

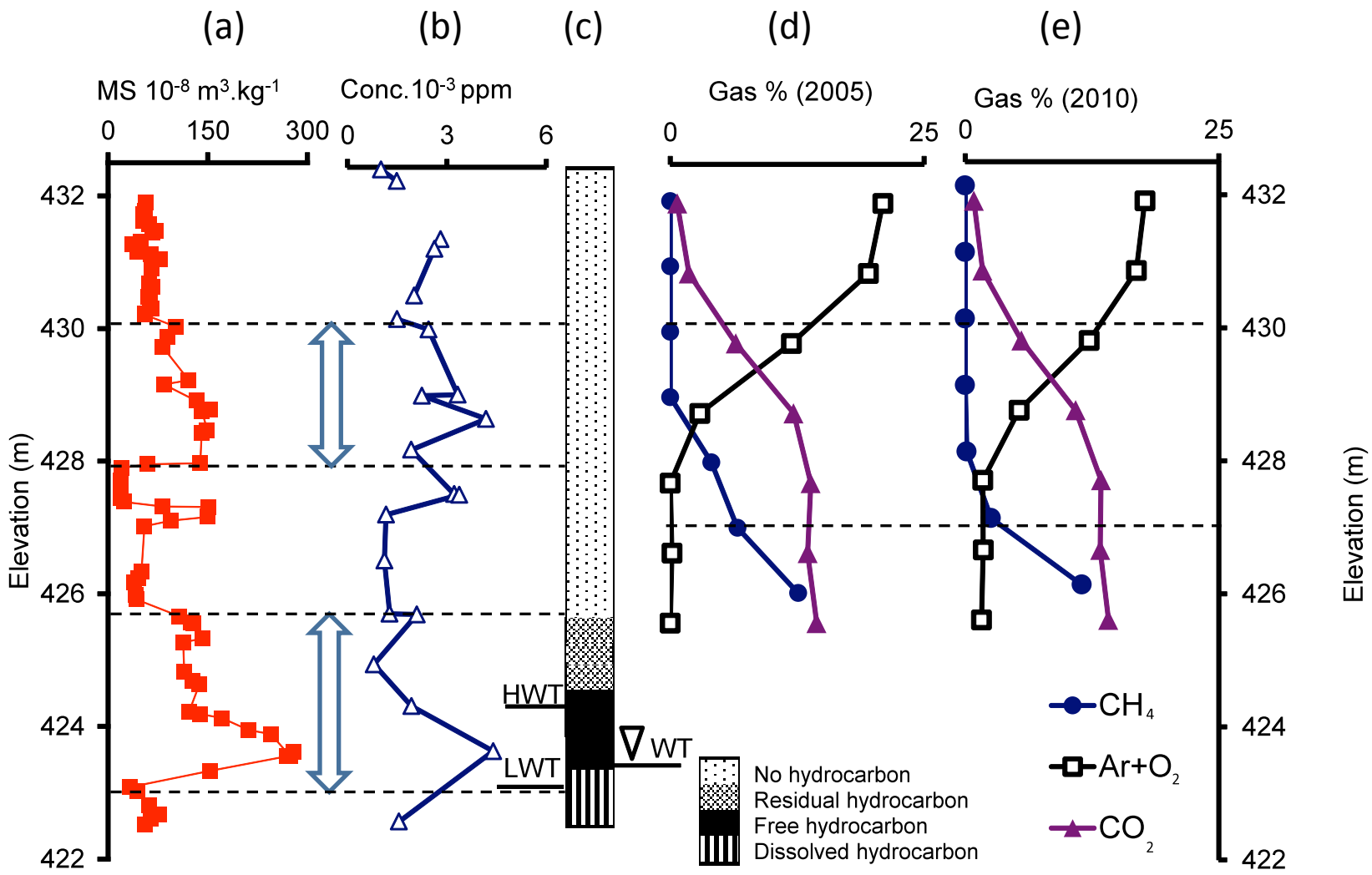
(a)
(b)
(c)
(d)
(e)
MS 10-8 m3.kg-1
0
150
300
Conc.10-3 ppm
0
3
6
Gas % (2005)
0
25
Gas % (2010)
0
25
Elevation (m)
432
430
428
426
424
422
HWT
LWT
WT
No hydrocarbon
Residual hydrocarbon
Free hydrocarbon
Dissolved hydrocarbon
CH4
Ar+O2
CO2
Elevation (m)

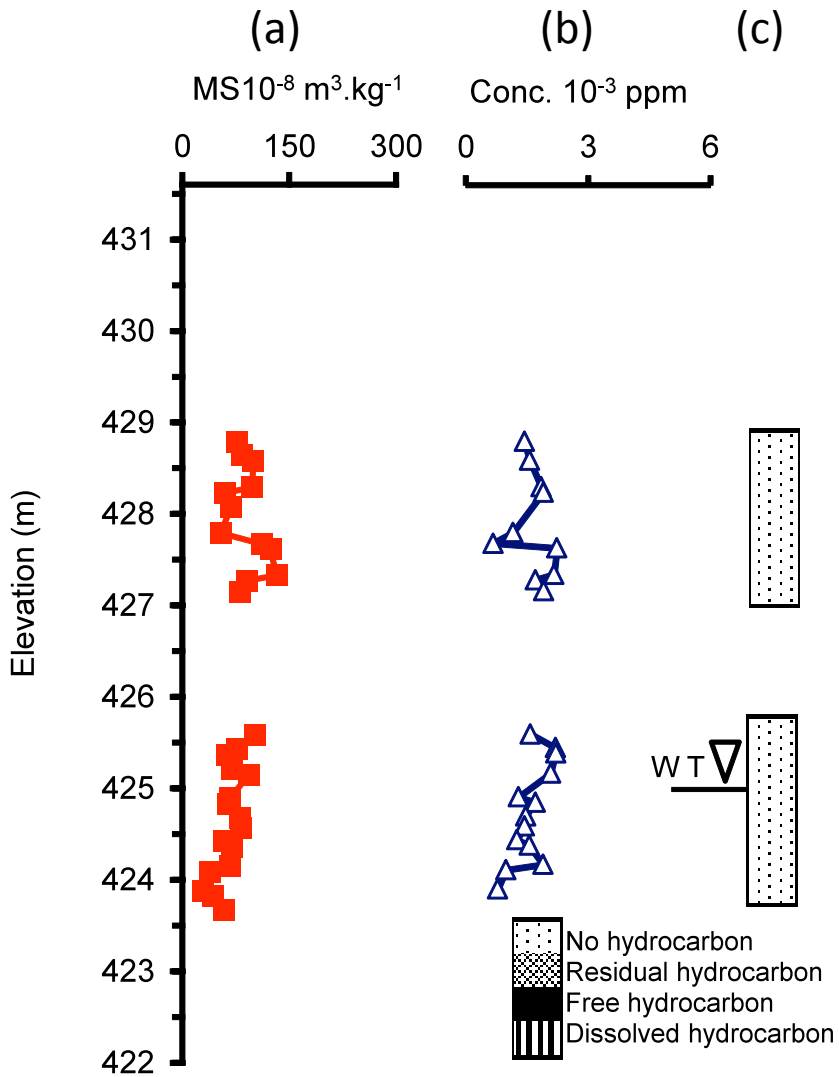
(a)
(b)
(c)
MS10-8 m3.kg-1
Conc. 10-3 ppm
0
150
300
0
3
6
Elevation (m)
431
430
429
428
427
426
425
424
423
422
W T
No hydrocarbon
Residual hydrocarbon
Free hydrocarbon
Dissolved hydrocarbon